MODELING SLIP BETWEEN A WEB AND A ROLLER

By

Benjamin D. Reish and Karl N. Reid
Oklahoma State University
USA

ABSTRACT

In roll-to-roll processes, slip between a web and a roller may be considered a defect. Slip can cause scratches which can be detrimental to a product, if not catastrophic. As line speeds increase to meet demands for more product per unit of operating time, the likelihood of slip increases. Slip may be partial or total, or a combination of both. In this paper we consider total slip only, i.e. slip over the entire area of contact between a web and a roller.

Whitworth [1] defined criteria for when full slip initiates, and developed a model for how slip affects the tension in the spans on either side of a roller where slip occurs. A Sliding Friction Driven Roller (SFDR) model is developed in this paper to account for the case where the web slides on the roller. The SFDR model uses the Whitworth criteria and span tension model. Both the Whitworth and SFDR models use the Capstan equation to determine if slip is occurring. With the Whitworth model, full adhesion of the web on the roller occurs until the torque which drives the roller, due to the tensions in the span on either side of the roller, reaches a critical level and slip initiates. But, with the SFDR model the torque which drives the roller is due to sliding friction between the web and roller.

The Euclid Web Line (EWL) in the Web Handling Research Center at Oklahoma State University was used to study slip both analytically and experimentally. A nonlinear dynamic model of the EWL was developed. Measured physical characteristics of the elements in the EWL were used in the analytical studies. Simulations for the case of a startup with an industrial ramp input in speed, showed that the Whitworth model is valid when the web and roller are moving at almost the same rotary speeds. However, simulations showed that the SFDR model covers the total slip situation when the tangential velocity of the roller and web velocity are distinctly different.

The simulations also showed that the torque due to bearing friction at a roller had to be equal to the torque due to the difference in tensions in the spans on either side of the roller in order for the initiation of slip to occur. Calculations using the measured bearing

friction on the roller of interest show that slip would not occur at speeds the EWL could attain.

In the experimental studies, a parasitic torque was applied to a roller mounted on load cells to create a slip condition. Hanging weights were used to apply the parasitic torque. An encoder was mounted on this roller to measure rotary velocity of the roller. Results from the experimental studies showed that the Whitworth model was valid only when the parasitic torque was small. In contrast, experimental studies showed that the SFDR model was valid only when the parasitic torque was large.

NOMENCLATURE

δ	-	Angle to the resultant force
θ_{in}	-	Angle on a roller to the incoming span
θ_{on}	-	Angle on a roller to the outgoing span
θ_{wn}	-	Angle of wrap on a roller
μ_n	-	Coefficient of friction between web and roller
ϕ	-	Ratio of web properties across the roller
A	-	Cross-sectional area of the web (width×thickness)
B_{fn}	-	Bearing friction
C_{mn}	-	Motor damping
C_{pn}	-	Dancer torsional damping constant
E	-	Young's Modulus
f_{qn}	-	Dancer input torque
GR_n	-	Gear Ratio between motor and shaft in contact with the web (number of shaft rotations per motor rotation)
Ind_n	-	Indicator storing the direction of slip
J_{mn}	-	Motor Inertia
J_{pn}	-	Dancer arm inertia
J_{sn}	-	Inertia of the shaft in contact with the web
K_{mn}	-	Motor constant
K_{pn}	-	Dancer torsional spring constant
L_{arm}	-	Dancer arm length
L_n	-	Free span length
l_{cg}	-	Dancer center of gravity location from pivot
m_p	-	Dancer mass
n	-	Index number (e.g., $n+1, n, n-1, n-2$)
R_n	-	Roller or roll radius
t_n	-	Tension in the web span
t_n^s	-	Slip tension
u_n	-	Current Input to the motor
$V_{n,0}$	-	Roller steady-state tangential velocities
v_n	-	Roller tangential velocity

INTRODUCTION

Slip may be partial or total, or a combination of both. This paper considers total slip only, i.e. slip over the entire area of contact between a web and a roller. Partial slip is an interface phenomena which is beyond the scope of this paper. When total slip occurs, the

instantaneous speed of the web is different than the surface speed or tangential speed of the roller. This idea is used later in this paper to develop a model for slip.

The factors involved in the initiation of total slip between a web and a roller have been studied in the past by Brandenburg [2] who set up the notation and theory using continuum mechanics. The region of contact is assumed to be divided into three regions – an entry region of slip, a region of adhesion, and an exit region of slip. Like Brandenburg, Whitworth [1] divides the region of contact on the roller where slip may occur into three regions. The roller where slip occurs is designated roller n, the incoming span as span $n-1$, and the outgoing span as span n. The continuity equations for spans $n-1$ and n are combined with Hooke's law, to develop an equation relating the tensions T_{n-1} and T_n and velocities v_n and v_{n+1}. From this equation, equations are developed for the region of adhesion and the region of slip. It is assumed that there is a temporary loss of adhesion between the web and the roller n, but that adhesion is maintained on rollers $n-1$ and $n+1$. When slipping occurs, the derivatives dT_{n-1}/dt and dT_n/dt are not defined. However, from dynamic considerations, T_{n-1} and T_n must be continuous functions of time. Using the Capstan equation leads to the following equations:

$$T_{n-1}^{s} = \frac{L_{n-1}^{eff} T_{n-1}^{ad} + L_{n}^{eff} \mathrm{T_n^{ad}}}{L_{n-1}^{eff} + L_{n}^{eff} e^{\mu_n \theta_{wn}}} \qquad \{1\}$$

$$T_{n}^{s} = T_{n-1}^{s} e^{\mu_n \theta_{wn}}$$

where L_{n-1}^{eff} and L_{n}^{eff} are the effective lengths of the incoming and outgoing spans considering the roller is slipping, $T_{n-1}^{ad}$and T_{n}^{ad} are the incoming and outgoing span tensions assuming adhesion on roller n, μ_n is the coefficient of friction between web and roller, and θ_{wn} is the wrap angle of the web on roller n. Equation {1} will be used in a slightly modified form later in this paper.

Ducotey and Good studied the effects of air entrainment on traction in [3]. No slip would be total traction while total slip would be no traction. Knowing characteristics of the web and roller, they were able to predict when total slip would occur. They developed a numerical method for the calculation of the coefficient of traction in [4]. In addition they studied the effects of web permeability and side leakage of air from between the web and roller on the thickness of the air film in [5]. They demonstrated that air film thickness is key to the prediction of total slip or loss of traction.

Dwivedula and Pagilla [6] proposed an alternate method for modeling slip which they argued would be better than that those previously developed when developing tension control schemes for web processing systems. Expressions were developed for an effective friction force and an effective normal force when the web is slipping over the entire region of contact between the web and roller. It was necessary to define and employ a traction model. A classical model of traction was selected, which included stiction, Coulomb friction, and viscous friction. The result is shown in Equation {2}.

$$v_{r,i} = v_i + \frac{t_i}{b}\left[1 - p\left(1 - e^{-\mu_i \theta_{wi}}\right) - \frac{t_{i+1}}{t_i}\right] \qquad \{2\}$$

where $v_{r,i}$ is the velocity of the roller, v_i is the velocity of the web, t_i is the tension in the incoming span, t_{i+1} is the tension in the outgoing span, θ_{wi} is the wrap angle, μ_i is the coefficient of friction of the web on the roller, and p and b are constants.

If the web is not slipping on the roller, $v_{r,i} = v_i$. But if the web is slipping on the roller, the velocity of the roller is generally less than that of web. The reduction in velocity of the roller is dependent on the incoming and outgoing tensions, the wrap angle and the coefficient of friction. Equation {2} was combined with the dynamic equation for the incoming web span to show the effects of slip on tension. Two conclusions were that when slipping occurs (i) there may be tension oscillations in the incoming and outgoing spans, and (ii) disturbances in the downstream span may propagate upstream.

THE EUCLID WEB LINE

The Euclid Web Line (EWL) is one of three major lines in the Web Handling Research Center at Oklahoma State University. The EWL was used to study slip both analytically and experimentally. Figure 1 is a photo of the EWL taken from the unwinding end. Figure 2 is a schematic diagram of the EWL. The line has four primary control sections: a dancer-controlled unwind, the s-wrap, the process section between the s-wrap and the pull roll, and the rewind. The unwind section is the focus of this paper. The EWL has capacity for up to a 16 inch wide web and up to 50 lbf of tension. Lateral guides are located on both the unwind and rewind ends to facilitate running the EWL forwards or backwards at web velocities up to 500 FPM. The idlers on this line are 3 inch diameter, steel sleeved rollers.

Figure 1 – Photo of the Euclid Web Line. The unwind section is in the foreground.

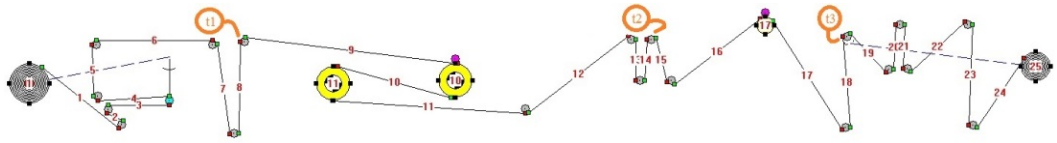

Figure 2 – Schematic diagram of the Euclid Web Line

MODELING AND MEASUREMENTS

Since the s-wrap section essentially isolates the unwind section from the process and rewind sections, the studies reported in this paper were limited to the unwind section. The unwind section contains one unwind roll, seven idlers, one dancer, and terminates at the lead s-wrap driven roller. It has nine free spans. The dynamic model used for simulating the unwind section is a coupled set of algebraic and differential equations. It is made specific by the parameters used in the models. For the simulations in this paper, the parameters have been measured, calculated from experiments, or found in documentation of the EWL and its components.

Unwind Roll and Motor Model

A physical model of the unwind roll and motor is shown in Figure 3.

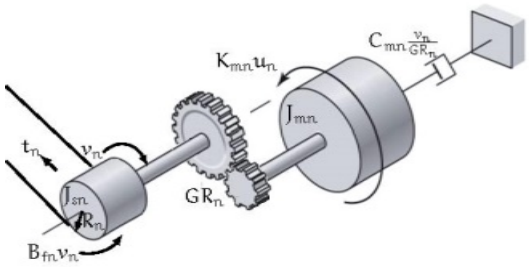

Figure 3 – Physical model of the unwind roll and motor (Adapted from [7])

The unwind roll and motor is modeled using a summation of moments about the spindle contacting the web. The result shown below.

$$J_n \frac{dv_n}{dt} = -(B_{fn} + C_{mn})v_n + \frac{R_n K_{mn} u_n}{GR_n} + R_n^2 t_n \quad \{3\}$$

where v_n is the tangential speed of the unwind roll and the gear ratio, GR_n, is defined as rotations of the shaft per rotation of the motor, and the inertia, J_n, includes the unwind roll inertia and the motor inertia reflected onto the shaft through the gear ratio. Referring to Figure 2, $n = 1$. The model, as shown, is linearized because it does not account for the unwind roll diameter decreasing as the line is operating. The change to nonlinear is not difficult in this case because the radius involved becomes a state of the system and the inertia of the roll is calculated from that state.

Rewind Motor Model

The rewind motor also is modeled as a summation of moments about the spindle contacting the web. Referring to Figure 2, $n = 25$. The result is

$$J_n \frac{dv_n}{dt} = -(B_{fn} + C_{mn})v_n + \frac{R_n K_{mn} u_n}{GR_n} - R_n^2 t_n \quad \{4\}$$

The Free Span Model

A physical model of the free span is shown in Figure 4. The free span of web is assumed in

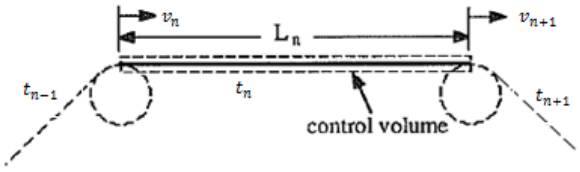

Figure 4 - Physical model of the free span with control volume indicated.

this paper to be linear-elastic, have constant cross sectional area, and undergo small strains. With these assumptions, it is demonstrated in [8] and [9] that the following nonlinear differential equation results from a combination of the law of conservation of mass for the control volume, and the application of Hooke's Law

$$L_n \frac{dt_n}{dt} = EA(v_{n+1} - v_n) + (v_n t_{n-1} - v_{n+1} t_n) \quad \{5\}$$

where t_n is the tension in the span of interest, t_{n-1} is the tension in the previous span (showing strain transport downstream), v_n is the speed of the roller at the entering end of the span, and v_{n+1} is the speed at the outgoing end of the span. The differential Equation {5} is nonlinear because of the multiplication of roller speeds and span tensions.

Idle Roller Model

A physical model of an idle roller is shown in Figure 5. The idle roller is modeled by taking a summation of moments about the idle roller's shaft which include the bearing friction and the torques applied by the two span tensions as shown below:

$$\frac{dv_n}{dt} = \frac{1}{J_n}\left(-B_{fn} v_n + R_n^2 (t_n - t_{n-1})\right) \quad \{6\}$$

where v_n is the tangential speed of the idler, t_n is the downstream span tension, and $t_{n-1}$is the upstream span tension.

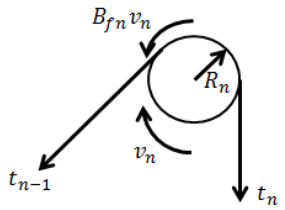

Figure 5 – Physical model of an idle roller

S-Wrap Roller Model

A physical model of an s-wrap roller is shown in Figure 6. The s-wrap roller is modeled by

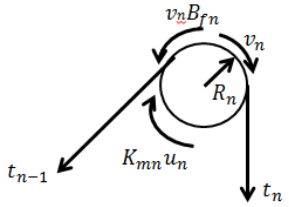

Figure 6 – Physical model of an s-wrap roller

taking a summation of moments about the roller's shaft, which include the bearing friction and the torques applied by the two span tensions, and the torque from the motor driving the s-wrap roll. The summation of moments is

$$J_n \frac{dv_n}{dt} = -(B_{fn} + C_{mn})v_n + \frac{R_n K_{mn} u_n}{G R_n} + R_n^2 (t_n - t_{n-1}) \quad \{7\}$$

where C_{mn} is the motor damping and K_{mn} is the motor torque constant.

Dancer Model

A physical model of the dancer system is shown in Figure 7.

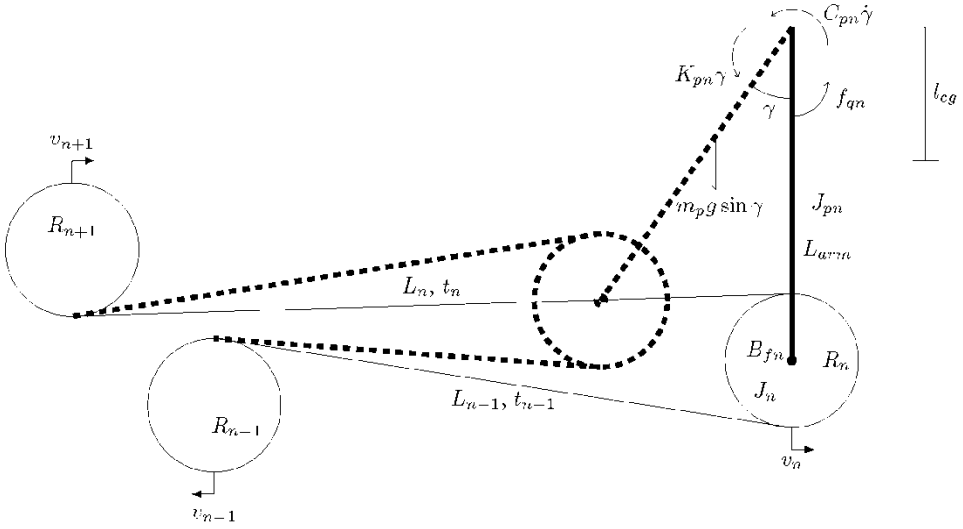

Figure 7 – Physical model of the dancer

The dancer is modeled by taking a summation of moments about the pivot of the pendulum and using modified free span models for the upstream and downstream spans. The summation of moments is

$$\frac{d^2\gamma}{dt^2} = \frac{1}{J_{pn}} \begin{bmatrix} -C_{pn}\dot{\gamma} - K_{pn}\gamma + f_{qn} - t_{n-1}(\mathrm{L_{arm}} + \mathrm{R_n}) \\ -t_n(\mathrm{L_{arm}} - \mathrm{R_n}) + m_p g l_{cg} \sin(\gamma) \end{bmatrix} \quad \{8\}$$

where $L_{arm} - R_n$ is the distance from the pivot to the point of contact of the dancer roller and the downstream span, $L_{arm} + R_n$ is the distance from the pivot to the point of contact

of the dancer roller and the upstream span, K_{pn} is the spring constant of the dancer and C_{pn} is the damping in the pivot of the dancer arm and torque application system, m_p is the mass of the pendulum dancer, and g is the gravity constant, and l_{cg} is the distance from the pivot to the center of gravity of the pendulum. The upstream and downstream free span models are modified to account for the effect of variable span length due to the swing of the pendulum:

$$L_{n-1}\frac{dt_{n-1}}{dt} = EA(v_n - v_{n-1}) + (v_{n-1}t_{n-2} - v_n t_{n-1}) + (EA - t_{n-1})\cdot \dot{L}_{n-1} \quad \{9\}$$

and

$$L_n\frac{dt_n}{dt} = EA(v_{n+1} - v_n) + (v_n t_{n-1} - v_{n+1}t_n) + (EA - t_n)\cdot \dot{L}_n \quad \{10\}$$

where these equations are indexed as if the dancer roller were n, and $\dot{L}_n$ is the time derivative of the n^{th} span length. Equations {9} and {10} are nonlinear, but can be linearized assuming small variations of all variables about a steady-state operating point, and by assuming that the pendulum angle γ is always sufficiently small such that sin $\gamma \approx \gamma$.

SLIP MODELS

Whitworth developed an approach to estimate the tensions in the spans upstream and downstream of a roller where slipping, occurs and defined criteria for determining if slip is occurring or not [1]. The criteria utilize the Capstan equation:

$$\left(\frac{t_n}{t_{n-1}}\right) = e^{(-\mu_n\theta_{wn})} \quad \{11\}$$

where n designates the nth roller, μ_n is the coefficient of friction of the web on the roller, and θ_{wn} is the wrap angle of the web on the roller. Rearranging Equation {11} and recognizing that it can be represented as two inequalities, results in the two criteria defined by Whitworth.

$$t_n - t_{n-1}e^{(-\mu_n\theta_{wn})} < 0 \quad \{12\}$$

$$t_n - t_{n-1}e^{(\mu_n\theta_{wn})} > 0 \quad \{13\}$$

Equation {12} indicates the case when the web speed is less than the roller speed and Equation {13} indicates the case when the web speed is greater than the roller speed. The upstream and downstream tensions for the case where there is slip are t_{n-1}^s and t_n^s respectively. A derivation involving the free span equations gives the results (modified versions of Equation {1}).

$$t_{n-1}^s = \frac{t_{n-1}L_{n-1} + \phi t_n L_n}{L_{n-1} + L_n\phi e^{Ind_n\,\mu_n\theta_{wn}}} \quad \{14\}$$

and

$$t_n^s = t_{n-1}^s e^{Ind_n\,\mu_n\theta_{wn}} \quad \{15\}$$

where $\phi = \frac{E_{n-1}A_{n-1}}{E_nA_n}$ and is the ratio of web properties across the roller number n, t_{n-1} is the tension in the incoming span assuming adhesion (which is replaced by t_{n-1}^s if a slip condition is true), L_{n-1} is the span length of the incoming span assuming adhesion

(instead of the L_{n-1}^{eff} as shown in [10]. Whitworth assumes $L_{n-1}^{eff} \approx \overline{L_{n-1}}$, the average span length, which he assumes is L_{n-1} in [1]), and Ind_n is the slip indicator taking a value of $-1, 0,$ or 1 based on Equations {12} and {13}. If Equation {12} is true, then $Ind_n = -1$. If Equation {13} is true, then $Ind_n = 1$. If neither Equations {12} nor {13} are true, then $Ind_n = 0$ [1]. Equations {14} and {15} are the results of strain matching the effective span length when the web is slipping to the strains determined when no slip condition is assumed to exist. Whitworth's model is a two-step process: first simulate an instant in time of a web process assuming no slip, then use the criteria to check for slip and adjust the span tensions if slip exists.

Ducotey and Good present a model in [3] and [4] that predicts a coefficient of traction between a web and a roller. The coefficient of traction depends on the air film thickness between the web and roller and the surface roughness of both the roller and the web. The model shows that the coefficient of traction virtually decreases to zero as the air film thickness increases. Once the air film thickness is large enough so that the traction becomes sufficiently small, no appreciable input torque is supplied by the web to the roller. In this case, a roller that is first spinning would spin down to a stop because of bearing friction alone.

The Sliding Friction Driven Roller (SFDR) Model

The Whitworth model is limited to the regime of slip where the change in span tension is affected by the additional length of the web in virtual contact with the roller. The Ducotey-Good model assumes an air film exits between the web and roller, which in the limit would allow for an effective disconnect of the web and roller. But, both the web and the roller have surfaces with asperities (roughness). Some level of adhesion due to contact between asperities is necessary if torque is to be transmitted from the web to the roller. If the air film thickness exceeds the asperities, torque can only be transmitted due to the viscosity of the air. This would be very small in a practical case.

The authors of this paper assumed that if the roughness of either the web or roller is sufficient, and the normal force between the web and roller is sufficient, torque will be transmitted through sliding friction. This assumption is the basis for the sliding friction driven roller (SFDR) model. The effects of slip are passed to the roller through decreases in the tension difference across the roller. A constant coefficient of friction between the web and roller and Whitworth's tension model are used in the SFDR. The result is a model for the roller during sliding as shown in the equations below (see Appendix for derivation of {16}):

$$F_n = -(-t_{n-1}^s \sin\theta_{in} + t_n^s \sin\theta_{on})/\cos\delta \qquad \{16\}$$

$$\frac{dv_n}{dt} = \frac{1}{J_n}\left(-B_{fn}V_n + Ind_n F_n \mu_{dn} R_n^2\right) \qquad \{17\}$$

where θ_{in} and θ_{on} are the incoming and outgoing span angles relative to the roller, δ is the angle to the resultant normal force which has to be determined based on geometry, μ_{dn} is the dynamic friction coefficient which is assumed to be equal to the static coefficient of friction, and Ind_n is the slip indicator used in Equations {14} and {15}. The indicator Ind_n indicates whether the sliding friction force is positive or negative on the roller. Otherwise, the roller model used is Equation {6}.

Some logic is needed to know when to switch between the sliding case and the non-sliding case. The Whitworth criteria are that logic. Equations {12} and {13} are used to select which case is present and when to switch. When the system or subsystem model is

being simulated, the Whitworth criteria are evaluated at every integration step. If slip is indicated, the SFDR model is used to define the friction force resulting from sliding contact rather than the model in Equation {6}.

Initial work on this project was accomplished using the **MATLAB** ode45 [11] integration routine with events defined for the switching of models. On the surface this sounds reasonable. But, the exactness with which **MATLAB** executes finding the time that the event occurs is problematic. To circumvent this problem, a Runge-Kutta 4 integration algorithm with fixed time steps was used when for simulations of the system model were performed.

Observations from the Model

One of the items of interest in looking at slip from a modeling perspective is when slip occurs. The Whitworth criteria only indicates when slip occurs and not how much, for example, the roller velocity decreases. The steady-state condition is one of those times when the initiation of slip may be indicated, i.e., when the roller velocity derivative is zero. But, there are times where an upset in either speed or tension causes the velocity derivative to be zero. It is this situation where slip can have its greatest impact. If the time derivative in Equation {6}, is set to zero, the equation becomes

$$B_{fn} v_n = R_n^2 (t_n - t_{n-1}) \qquad \{18\}$$

So bearing friction can cause slip to initiate. Barring other disturbances, lower bearing friction means higher line speeds with no slip. Solving Equation {18} for the speed of the roller and using estimated values for bearing friction, shows that the EWL would have to run in excess of 1200 FPM for slip to become a problem at the assumed tension levels.

EXPERIMENTAL STUDIES

Experiments were performed on the Euclid Web Line (EWL). The experiments included idler speed tracking with a parasitic torque applied to the idler, evaluation of the coefficient of friction between the web and roller before and after the surface was treated, and idler bearing friction determination.

Parasitic Torque

The EWL can operate at line speeds up to 500 FPM. Slip could not be detected at any speed up to and including 500 FPM. A parasitic torque was applied to roller 9 (Figure 2) to cause slip at line speeds feasible for the Euclid line. Figure 8 shows the experimental setup where a piece of cloth was draped over the roller and weights were suspended from the cloth to apply a known tension. The difference between the tension meter reading and the hanging weights was assumed to be the force applied to the roller in addition to its normal bearing friction. A wheel encoder was used to capture the speed of the roller during each run. The encoder had very little bearing friction compared to the idler.

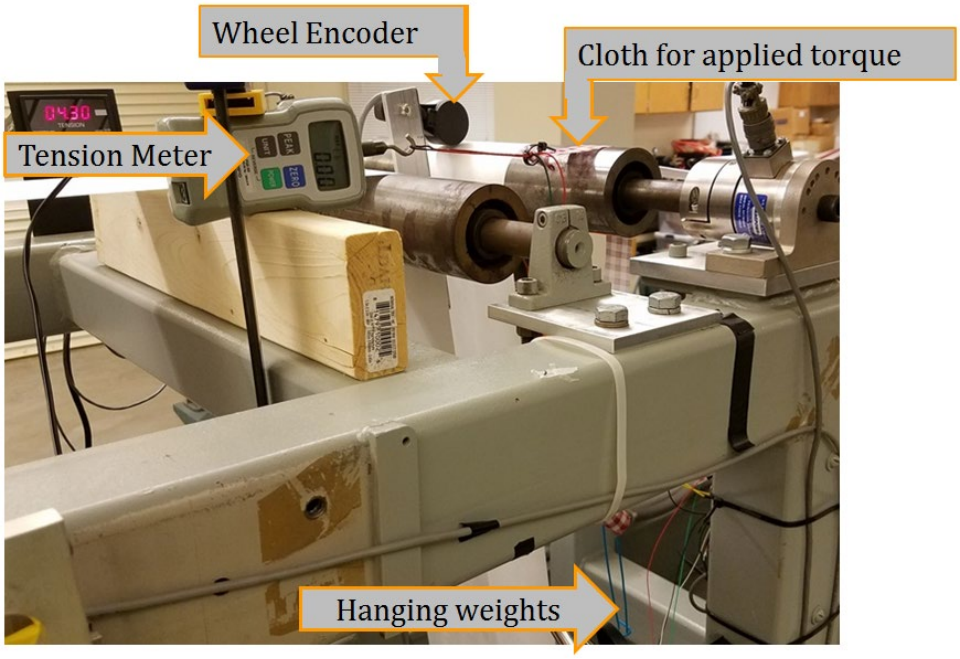

Figure 8 – Induced slip setup on Euclid Web Line caused slip to occur at attainable speeds.

With the parasitic torque added to roller 9, the EWL was run through a start-up from 0 to 400 FPM, held at 400 FPM for about 80 seconds and then shutdown. The force meter was read after the line speed reached 400 FPM. The hanging weight was recorded for each run and the roller speed was captured with the wheel encoder. Traces of idler speed as indicated by the wheel encoder are shown in Figure 9. Between 0 and 1.745 lbf hanging weight, no slip is evident in the idler speed. The parasitic torque causes slip at 2.245 lbf. Higher hanging weights cause the idler to attain lower quasi-steady-state speeds until at 2.569 lbf, the idler stops several times during the steady running at 400 FPM. With that much hanging weight, the idler did not reach 100 FPM before slowing down. Hanging weights up to 3.379 lbf were applied, but above 2.569 lbf, the results were similar to that of the idler with 2.569 lbf hanging weight.

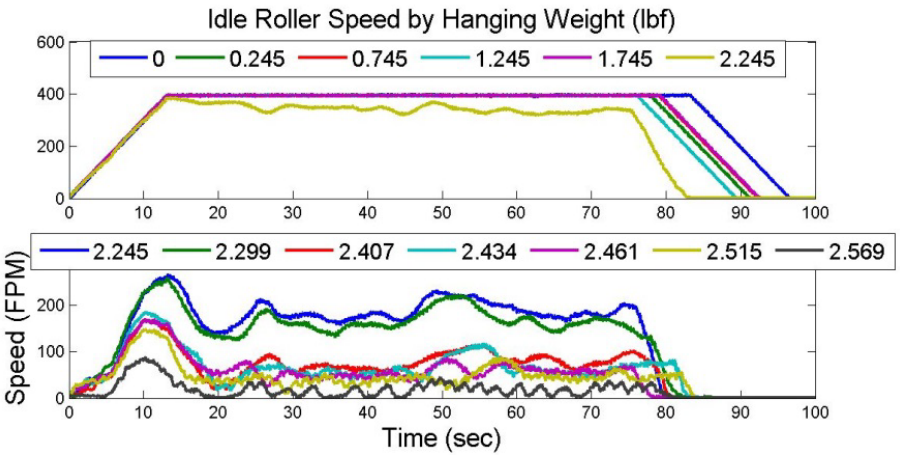

Figure 9 – Traces of the idler speed as indicated by the wheel encoder. Slip initiates with a hanging weight of about 2.2 lbf and the idler comes to rest with a hanging weight of about 2.56 lbf.

Determining Coefficient of Friction between Web and Roller

Since the coefficient of friction of the web on the roller is important to the SFDR model, the surface finish of the idler was examined. The roller was original equipment with the line and it had become rusty. Also, the coefficient of friction is important to the SFDR model, so a

Figure 10Figure 10

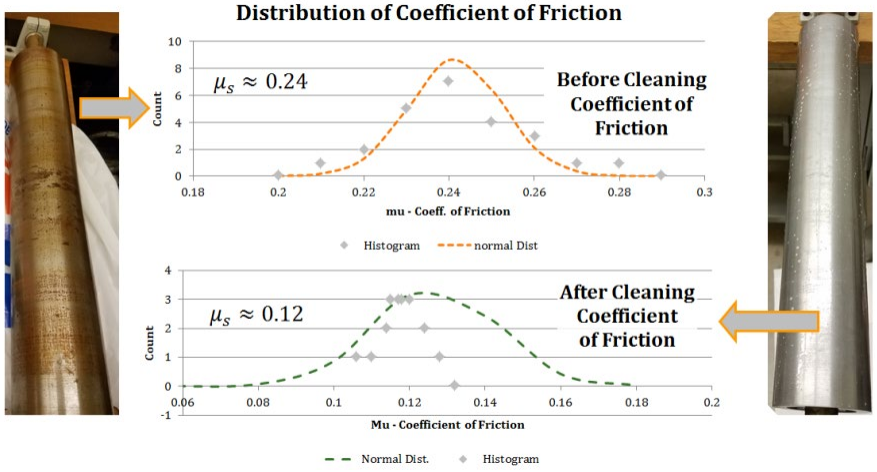

Figure 10 – The difference a rust free roller makes in coefficient of friction is 50%.

coefficient of friction experiment was accomplished in accordance with the method described by R. J. Lynch [12]. The average coefficient of friction of the original roller was 0.24. The post cleaning result was 0.12. Figure 10 shows the before and after rust removal idler photos and the coefficient of friction test results.

Parasitic Torque Experiments – Post Rust Removal

With the parasitic torque added to the rust free idler 9, the EWL was run through a start-up from 0 to 400 FPM, held at 400 a FPM for about 80 seconds, and then shutdown. The force meter was read after the line speed reached steady 400 FPM. The hanging weight was recorded for each run and the roller speed was captured with the wheel encoder. Traces of idler speed as indicated by the wheel encoder are shown in Figure 11. The idler speed indicates that slip initiated with only 1.419 lbf hanging weight instead of 2.245 lbf before rust removal. The idler came to rest during the run with a hanging weight of only 1.568 lbf instead of 2.569 lbf as before. The results in Figure 9 and Figure 11 show that when the primary mechanism for providing torque to an idler is sliding friction, the better the surface finish the more likely slip will occur at that idler at lower line speeds.

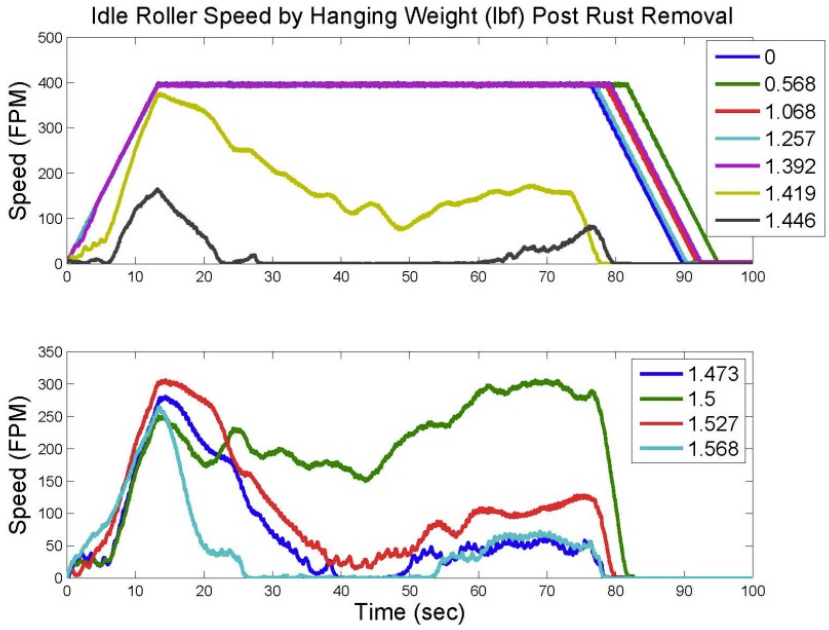

Figure 11 – Idler speed post rust removal with varying parasitic torques shows that slip initiates at about 1.4 lbf and the idler comes to rest during the run with about 1.56 lbf hanging weights.

Bearing Friction Experiment

The bearing friction of the idler was evaluated using a spin-down test as described in [12]. Two cases were considered - when the bearing was cold and then after running the line for 10 minutes. Figure 12 shows the "cold" and "warm" spin-down speed traces from the wheel encoder. Four runs were made for each case. Different initial speeds were used in order to separate the traces so the general character could be seen. The final speed for all traces in Figure 12 was 200 FPM. Two types of models were considered to represent the spin down tests – a viscous friction based model and a Coulomb friction based model.

A roller mounted on bearings which provide a resisting torque that is a simple function of rotary speed, can be modeled as a first order linear system as shown by the following equation,

$$I\dot{\omega} + c\omega = 0 \qquad \{19\}$$

where I is the rotary inertia, c is the rotary viscous coefficient, $\dot{\omega}$ is the rotary acceleration of the roller, and ω is the rotary speed of the roller. The solution of this differential equation is

$$\omega = \omega_0 \, e^{-(c/I)t}$$

where ω_0 is the value of ω when $t = 0$. This solution is the decreasing exponential shown by the blue dot-dashed curves ("viscous frict.") in Figure 12.

All four experimental traces for each case in Figure 12 have an almost constant negative slope. That is, the deceleration rate is nearly constant. An appropriate model of this behavior is that rotary speed is a simple function of time, $\omega = -Kt$. In this equation, ω is the rotary speed of the roller, K is a constant, and t is time. This model represents the spin down data the best. And, it is this behavior that suggests that the resisting torque in the spin down tests of the roller is due primarily to Coulomb friction rather than viscous friction in the bearings.

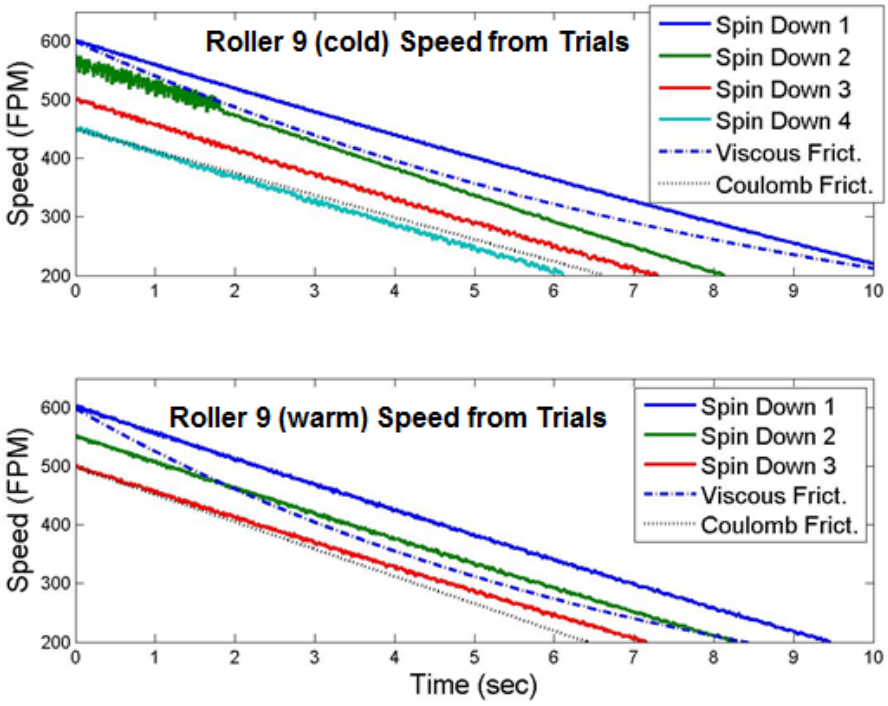

Figure 12 – Spin-down test speed traces are used to calculate the viscous bearing friction. The viscous friction simulation does not track the experimental data well for either the "cold" or "warm" bearings. A Coulomb friction model matches the deceleration rate reasonably well.

SIMULATION RESULTS

The Sliding Friction Driven Roller (SFDR) model is used to simulate some of the runs from the experimental section. The results drive the surface finish and the bearing friction studies discussed above.

The SFDR Model with Parasitic Torque

The conditions of the Parasitic Torque experiment were simulated using both the Whitworth model and the SFDR model. The Whitworth model shows the limiting characteristic in Figure 13 when it (red line) drops about 50 FPM with 3.379 lbf simulated hanging weight while the experimental data shows that the idler was stopped with that level of hanging weight. The SFDR model with 1.7 lbf hanging weight tracks up the ramp, but then shows slip as it settles in on the speed of the 2.245 lbf hanging weight experiment. These two weights bracket the beginning of slip in the experiment so the model showing slip is not terrible. The black line in Figure 14 shows the SFDR model with 2.515 lbf hanging weight simulated and it hits the experimental speed after slipping. The miss with 1.7 lbf hanging weight in the model causes the testing of the coefficient of friction between web and roller and the bearing friction study to define parameters.

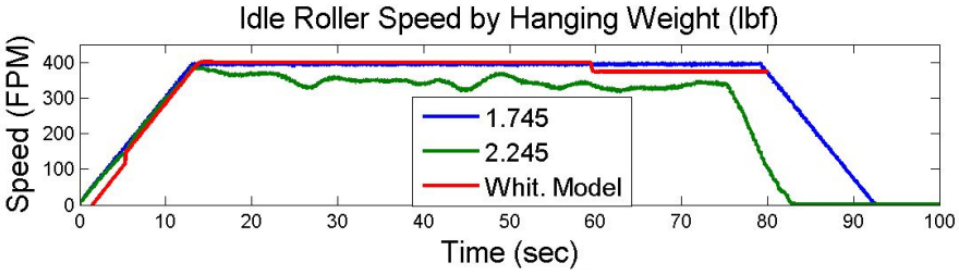

Figure 13 – To illustrate a limit in the Whitworth model, the blue line is experimental data with no slip, the green is with slip, and the red line is simulation data using only the Whitworth model and 3.379lbf hanging weight. The Whitworth model only allowed about a 50FPM drop in speed while the experimental data for that hanging weight was stopped.

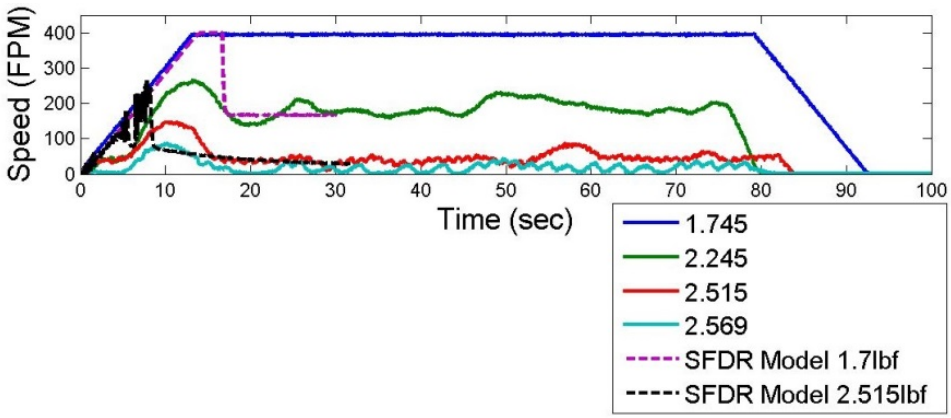

Figure 14 – SFDR model plotted against experimental data. The hanging weight in the simulation seems to impact when slip initiates and what speed is finally attained. At the lighter hanging weights, the SFDR model shows slip where there is not any, but as heavier hanging weights are applied, the SFDR does a good job of settling in on the slipping speed of the idler (see the black dotted line overlaying the red line).

Surface Finish and Bearing Friction Impacts

These experiments refined parameter values in the simulation models. There was a little simulation in the bearing friction study to cross-check the evaluated bearing friction with the experimental data. As Figure 12 showed with the dashed and dotted lines, the viscous model of friction does not follow the experimental data which lead to the creation of a Coulomb friction model for the Euclid Web Line's bearing friction.

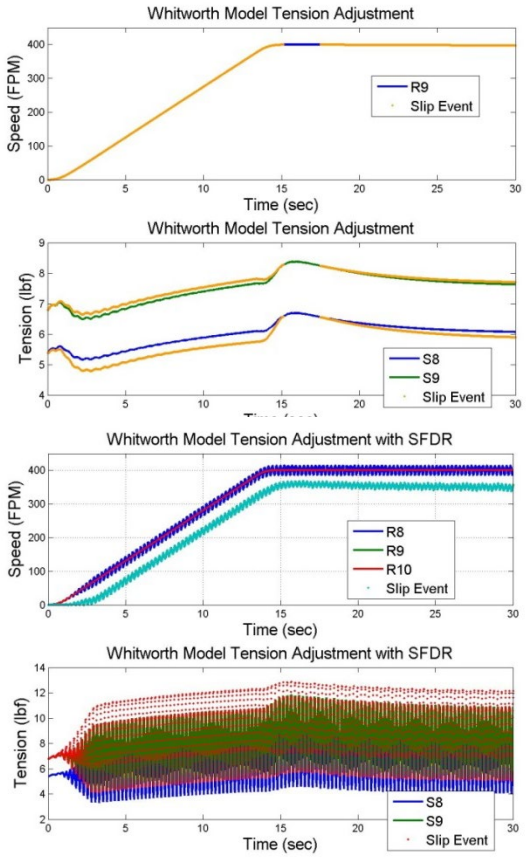

Figure 15 – The Whitworth model shows little variation in speed due to slip while the SFDR model predicts a 50 fpm decrease in speed with a 1.419 lbf parasitic torque applied. The experimental data for this situation shows the idler speed dropping throughout the run.

Applying the results of the coefficient of friction study and the bearing friction study to the simulations gives Figure 15. On the left is the Whitworth model output for roller 9 speed and
spans 8 and 9 tensions with 1.419 lbf hanging weight applied. The speed difference due to slip is unnoticeable. On the right, the SFDR model with the same set of parameters and hanging weight shows a 50 FPM average decrease in speed. For reference, see Figure 11 for what the EWL did with 1.419 lbf hanging weight. It did not run at 400 FPM, but it decreased more than 50FPM, too.

CONCLUSIONS

This paper has shown the required differential equations for simulating the unwind section of the Euclid Web Line. Two slip models are discussed, (i) Whitworth's model and criteria and (ii) the Sliding Friction Driven Roller (SFDR) model. An experiment

was conducted that involved adding a parasitic torque to a roller in order to create a slip condition while running the EWL at speeds that were achievable.

Comparison of the simulations with results from the experimental studies showed that the Whitworth model was valid only when the parasitic torque was small. In contrast, experimental studies showed that the SFDR model was valid only when the parasitic torque was large.

The Whitworth model covers the initiation of slip while the SFDR model covers the slip situation where the roller speed is distinctly different than the web speed. A model is needed to cover the entire spectrum. Such a model is expected to be heavily dependent on the contact mechanics between the web and the roller.

REFERENCES

[1] Whitworth, D. P. D., Tension Variations in Pliable Material in Production Machinery, 1979.

[2] Brandenburg, G., "New Mathematical Models for Web Tension and Register Error," in Proc. 3rd International IFAC Conf. on Instrumentation and Automation in the Paper, Rubber, and Plastics Industries, Brussels, 1976.

[3] Ducotey, K. S., and Good, J. K., "Predicting Traction in Web Handling," Transactions-American Society of Mechanical Engineers Journal of Tribology, Vol. 121, 1999, pp. 618-624.

[4] Ducotey, K. S., and Good, J. K., "A Numerical Algorithm for Determining the Traction between a Web and a Circumferentially Grooved Roller," Journal of Tribology, Vol. 122, 2000, pp. 578-584.

[5] Ducotey, K. S., and Good, J. K., "The Effect of Web Permeability and Side Leakage on the Air Film Height between a Roller and Web," Transactions-American Society of Mechanical Engineers Journal of Tribology, Vol. 120, 1998, pp. 559-565.

[6] Dwivedula, R. V., and Pagilla, P. R., "Modeling of Web Slip on a Roller and its Effect on Web Tension Dynamics," in 2005 ASME International Mechanical Engineering Congress and Exposition, Orlando, FL, 2005.

[7] W. Palm, System Dynamics, New, York: McGraw-Hill, 2014.

[8] Shin, K.-H., "Distributed Control of Tension in Multi-Span Web Transport Systems," Oklahoma State University, Stillwater, OK, 1991.

[9] Reid, K. N., and Lin, K.-C., "Control of Longitudinal Tension in Multi-Span Web Transport Systems During Start-up," Proceedings of the Second International Conference on Web Handling, June 1993, pp. 77-95.

[10] Whitworth, D. P. D., "Tension Variations in Pliable Material in Production Machinery," Applied Mathematical Modelling, Vol. 7, No. 3, 1983, pp. 189-196.

[11] MATLAB, Natick, Massachusetts, United States: The MathWorks, Inc., 2013.

[12] Lynch, R., Private Communications, 2018, pp. Tab 1-2.

[13] Shin, K.-H., "Distributed Control of Tension in Multi-Span Web Transport Systems," 1991.

APPENDIX

The SFDR model requires a friction force to be applied at the periphery of the idle roller. Coulomb friction was assumed.

$$F_f = \mu_n F_n \quad \{20\}$$

A simple static force balance was applied to an idle roller to define an average resultant normal force for calculating the friction force. The normal force is assumed to bisect the wrap angle of the roller giving $\delta = \theta_{on} + \theta_{wn}/2 + \pi$.

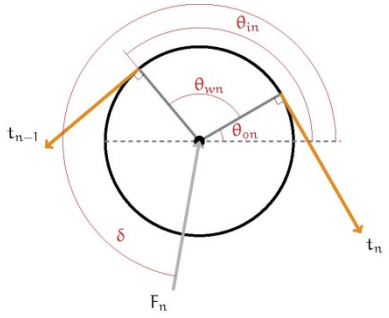

Figure 16 – Force balance on a roller

Then the summation of forces in the horizontal direction is

$$(-t_{n-1}) \sin\theta_{in} + t_n \sin\theta_{on} + F_n \cos\delta = 0 \quad \{21\}$$

$$F_n = -(-t_{n-1} \sin\theta_{in} + t_n \sin\theta_{on})/\cos\delta \quad \{22\}$$

The resultant force F_n is assumed to be approximately the normal force on the roller due to the web.